analytical chemistry

Article

pubs.acs.org/ac

Fluorescent Nanoconjugate Derivatives with Enhanced Photostability for Single Molecule Imaging

Daniel T. Reilly,[†] Sung Hoon Kim,[‡] John A. Katzenellenbogen,[‡] and Charles M. Schroeder*[,†,‡,§]

[†]Department of Chemical and Biomolecular Engineering, University of Illinois at Urbana−Champaign, Urbana, Illinois 61801, United States

[‡]Department of Chemistry, University of Illinois at Urbana−Champaign, Urbana, Illinois 61801, United States

[§]Center for Biophysics and Quantitative Biology, University of Illinois at Urbana−Champaign, Urbana, Illinois 61801, United States

Supporting Information

ABSTRACT: Fluorescence-based imaging techniques critically rely on bright and photostable probes for precise detection of biological molecules. Recently, a new class of multichromophoric probes based on fluorescent dendrimer nanoconjugates (FDNs) was developed for single molecule fluorescence microscopy (SMFM). FDNs are generated by covalent conjugation of multiple fluorescent dyes onto macromolecular polymeric scaffolds and show marked increases in brightness and long-term photostability relative to their single organic dye constituents. Multichromophoric probes, however, are generally known to suffer from transient fluorescence emission intensities and long excursions into dark states. To overcome these issues, photostabilizers can be added to bulk solution, though some small molecule additives may exhibit poor aqueous solubility or biological toxicity. In this work, we develop enhanced FDN derivatives by covalently linking a redox-active photostabilizer (Trolox) directly onto FDN molecular scaffolds. In one approach, multiple organic dyes (Cy5) and Trolox molecules are randomly distributed on dendritic scaffolds in tunable stoichiometric amounts, and in a second approach, Cy5 dyes are covalently linked to Trolox in a precise 1:1 stoichiometry followed by covalent attachment of Cy5−Trolox conjugates onto dendrimers. In all cases, FDN−Trolox conjugates show increases in photostability, brightness, and reduced fluctuations in transient fluorescent intensity relative to FDN probes. Bulk and single molecule photophysical data for FDN probes are compared to single self-healing dye systems such as Cy5−Trolox, and as a proof-of-principle demonstration, we use FDN−Trolox derivatives for bulk immunofluorescence imaging. Overall, our work suggests that self-healed multichromophoric systems such as FDN−Trolox probes present a useful strategy for increasing fluorescent probe photostability.

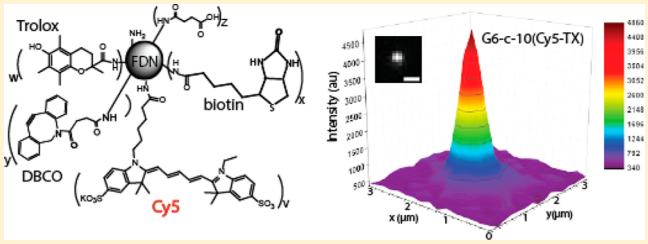

Single molecule fluorescence techniques allow for the direct observation of biological processes, thereby providing a window into viewing molecular-level phenomena. Fluorescence imaging with high spatial and temporal resolution critically relies on bright and photostable fluorescent probes, which provide increased sensitivity for biological imaging and molecular identification. To this end, advances in molecular probe development have opened up new vistas in single molecule fluorescence imaging, allowing for subcellular events to be visualized at unprecedented spatial resolution in the nanometer size range.[1−3] Organic dyes such as cyanine family dyes (e.g., Cy3 or Cy5) and near-infrared emitting dyes (e.g., Cy7 or Alexa750) can be used as relatively nonperturbative fluorescent labels due to their small molecular-scale size.[4,5] However, the vast majority of organic dyes suffers from two major drawbacks: rapid irreversible photobleaching, which limits the effective photon count from single molecules, and transient fluctuations in intensity, including intermittent bright/dark states (i.e., blinking),[6,7] which complicates the study of dynamics at the molecular level.[8]

Transient conversion into dark states can be caused by several different photophysical and photochemical mechanisms. Organic dyes with internal π-bond conjugation such as the cyanine series have been shown to transition to short-lived (microseconds) intermittent dark states due to cis/trans isomerization.[9,10] In addition, intersystem crossing from an excited singlet (S_1) to a nonfluorescent triplet state (T_1) can also result in dark states (microseconds to milliseconds).[11,12] In some cases, even longer-lived dark states (milliseconds or longer) have been shown to occur due to oxidation/reduction reactions of dyes in excited states with redox-active partners in solution.[13] Moreover, the red-emitting dye Cy5 has been shown to exhibit long-lived, reversible dark states via Michael addition with a primary thiol or phosphine, forming an adduct on the polymethine bridge and breaking π-conjugation, which has proven useful for super-resolution imaging.[14−17] Nevertheless, potential damage to organic dyes resulting in irreversible

Received: August 9, 2015
Accepted: October 12, 2015
Published: October 13, 2015

DOI: 10.1021/acs.analchem.5b03059
Anal. Chem. 2015, 87, 11048−11057

photobleaching is generally associated with conversion to triplet states, which has strongly motivated the development of photostabilizers to quench triplet states and improve the performance of organic dyes in solution.[18]

A general strategy to improve the photostability of organic dyes involves the addition of antifading reagents or photostabilizers to solution. These are designed to restore the ground singlet state by quenching triplet states or scavenging radical species to prevent chemical damage to fluorophores. In many cases, oxygen is removed from solution using coupled enzymatic systems such as glucose oxidase−catalase (GOC)[19] or protocatechuic acid−protocatechuate-3,4-dioxygenase (PCA/PCD),[20] which prevents the formation of reactive oxygen species (ROS) that can cause irreparable damage to organic dyes. However, oxygen serves as a triplet state quencher, so enzymatic removal of oxygen also tends to increase the conversion into dark triplet states.[21,22] One of the first protective agents used in single molecule experiments to suppress photobleaching is the reducing agent β-mercaptoethanol (βME).[23] More advanced protective agents such as triplet state quenchers (TSQs) such as cyclooctatetraene (COT), nitrobenzylalcohol (NBA), or redox-active compounds such as Trolox (TX) or ascorbic acid (AA) and methyl viologen (MV) are typically added to solution as photostabilizing reagents in conjugation with oxygen scavenging systems.[24−29] To this end, addition of a reducing and oxidizing system (ROXS) such as AA and MV can be used to quench effectively triplet states and improve the photostability of organic dyes such as Cy5.[30,31] However, solution-based addition of TSQs or ROXS requires relatively high concentrations in the millimolar range, which could perturb innate biological function or be toxic to living cells.[32]

To circumvent potential issues associated with solution-based additives, a series of "self-healing" fluorophore derivatives was recently developed by covalently linking TX, 4-nitrobenzyl alcohol (NBA), or COT directly onto the cyanine dye Cy5.[33,34] For these organic dye derivatives, the close proximity of a redox-active species or TSQ increased the local concentration of photostabilizers, thereby promoting molecular collisions and effectively quenching triplet states. Self-healing dye derivatives were observed to exhibit large increases in average time spent in a bright or "on" state, along with increased bulk photostability. The mechanism of self-healing cyanine dyes was subsequently explored using single molecule methods.[35,36] In the case of Cy5−TX derivatives, the quenching mechanism is thought to involve the sequential reaction of the triplet state dye with the reducing agent TX to form a radical anion dye and radical cation TX, followed by rapid oxidation of the dye with the TX radical cation. This series of redox reactions regenerates a self-healed ground state dye and TX in a "ping-pong" photocatalytic cycle. The general strategy was extended to self-healing dyes spanning the visual spectrum using a similar conjugation scheme with Cy2, Cy3, Cy3.5, Cy5, Cy5.5, and Cy7.[37]

Moving beyond self-healing organic dye derivatives, there is a need for development of new fluorescent probes with combined increases in photostability and brightness, thereby allowing for precise fluorescence detection of biomolecules. To this end, a series of probes known as fluorescent dendrimer nanoconjugates (FDN) was recently developed for single molecule imaging.[38] FDN probes are multichromophoric organic dye conjugates based on polyamidoamine (PAMAM) dendrimers, which are macromolecular in size (∼2−5 nm) and generally smaller than inorganic quantum dots and exhibit a high degree of water solubility.[39] Dendritic polymers provide a versatile molecular scaffold for direct conjugation of multiple fluorescent dyes (such as Cy3 or Cy5) and chemical moieties for subsequent conjugation and biomolecular labeling. In prior work, FDN probes containing 8 Cy5 dyes showed a ∼4× increase in average brightness compared to single Cy5 dyes. In addition, Cy5−FDNs showed a ∼6−10× increase in long-term photostability (duration of time to irreversible photobleaching) compared to a single Cy5 dye, thereby providing substantial increases in total photon output over the lifetime of an FDN probe.[38]

Although FDN probes show enhanced brightness and long-term photostability relative to their constituent single organic dyes, FDN probes are multichromophoric systems with close spatial proximity of dyes, which can result in complex photophysics.[40] Multichromophoric systems have been shown to exhibit transient and dynamic fluorescence emission intensities at the single molecule level,[41] including hydrophobic, aromatic dendrimer systems containing multiple fluorescent dyes.[42,43] Single FDN probes were observed to show transient fluorescence emission, with broad unstructured peaks and long excursions (hundreds of milliseconds) into dark states, which complicates the use of FDN probes in single molecule fluorescence experiments. Interestingly, addition of the redox-active photostabilizer TX into solution (in millimolar amounts) substantially decreased the transient fluctuations in the fluorescence emission trajectories of single FDN probes, which suggests that photostabilizers such as TSQs and redox-active compounds could play a key role in further enhancing the photostability of multichromophoric fluorescent probes despite the complex photophysics.

In this paper, we report the development of multichromophoric FDN derivatives with covalent attachment of the photostabilizer TX. We synthesized two different versions of these FDN derivatives: (1) r-FDN−TX probes containing multiple Cy5 dyes and multiple TX molecules randomly distributed on the dendrimer surface, which allows for control over the average stoichiometric loading and ratio between Cy5 and TX, albeit without precise control over the spatial distribution of Cy5 and TX molecules, and (2) c-FDN−TX probes containing Cy5−TX conjugates directly linked to the dendrimer surface, thereby yielding controlled physical spacing between Cy5 dyes and photostabilizer molecules on the dendritic scaffold. Using this approach, we generated a series of r-FDN−TX and c-FDN−TX derivatives, and we characterized the photophysical properties of these multichromophoric probes using single molecule fluorescence microscopy (SMFM). We observe that direct covalent attachment of TX to FDN probes generally stabilizes the transient fluorescence emission of single probes, and we explore the role of the spatial arrangement of dye and photostabilizer molecules on the photostability for FDN−TX probes with comparisons to single Cy5−TX conjugates. Finally, FDN−TX derivatives are used in proof-of-principle immunofluorescence imaging experiments to highlight applications to biological systems, along with specific labeling of DNA for single molecule imaging and detection.

EXPERIMENTAL SECTION

Synthesis of FDN and Cy5−TX Compounds. Amine-reactive Cy5−NHS ester dyes were synthesized as previously described[44] and directly conjugated to generation 5 and generation 6 (G5, G6) PAMAM-amine terminated dendrimers (Supporting Information). G5 and G6 PAMAM dendrimers

DOI: 10.1021/acs.analchem.5b03059
Anal. Chem. 2015, 87, 11048−11057

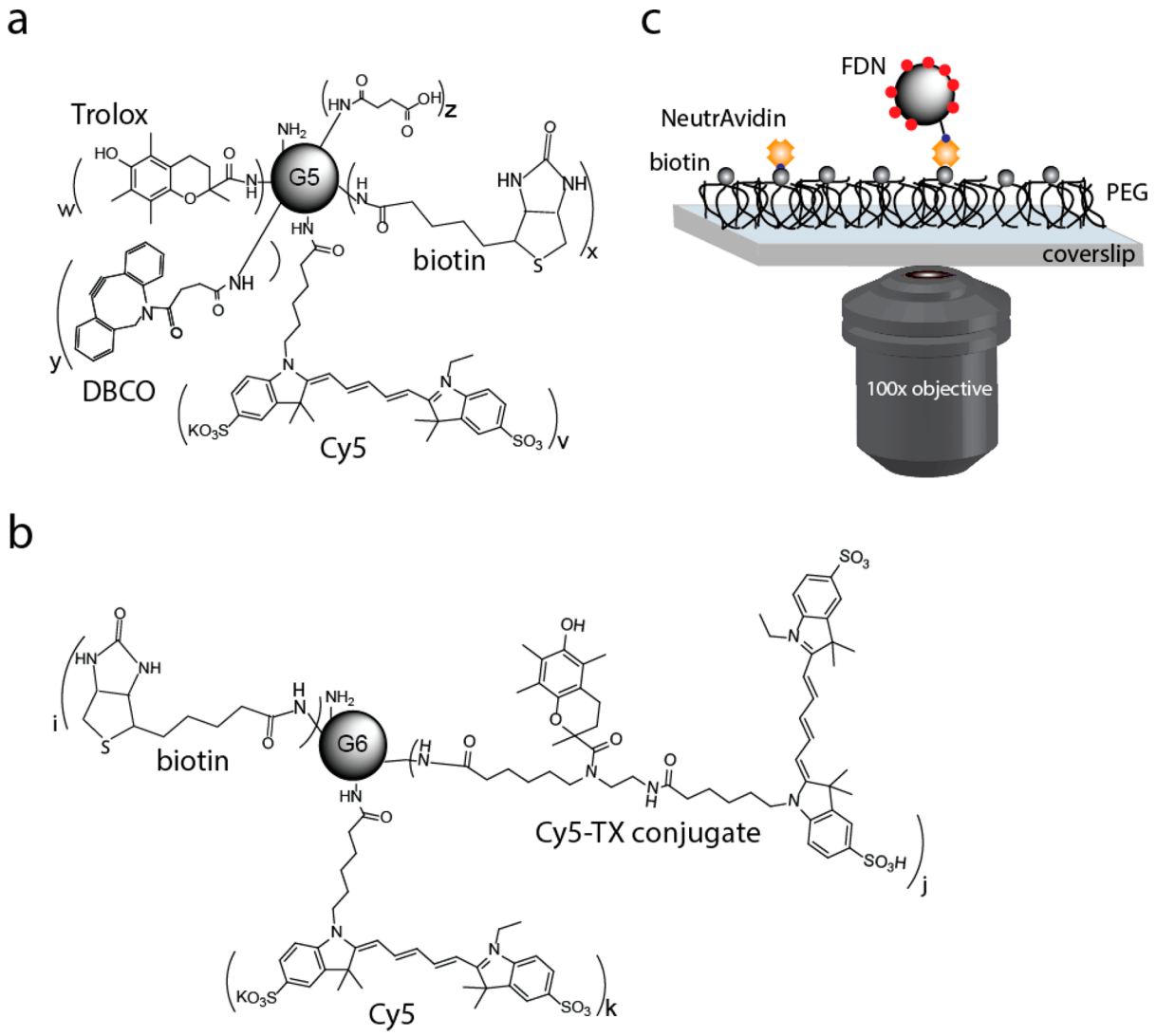

Figure 1. Fluorescent dendrimer nanoconjugates for single molecule imaging. (a) Schematic of chemical structure of random addition FDN probes (r-FDN and r-FDN−TX). Values for *v*, *w*, *x*, *y*, *z* for all samples are reported in Table S1. The sphere represents the G5 PAMAM dendrimer (not to scale); for more structural detail, see Figure S1. (b) Schematic of chemical structure for controlled addition FDN probe (c-FDN and c-FDN−TX). Values for *i*, *j*, *k* are reported in Table S2. (c) Schematic of in vitro single molecule characterization experiments. Coverslips are coated PEG/PEG−biotin, with fluorescent probes attached through biotin NeutrAvidin linkages.

nominally contain 128 and 256 surface primary amines, respectively, allowing for facile chemical reaction with a variety of NHS−ester substituents. Dendrimers were labeled with either biotin for biotin−avidin affinity labeling or dibenzocyclooctyne (DBCO) for strain-promoted copper-free click chemistry labeling.[45,46] For the indicated samples, an NHS-activated form of Trolox (TX) was prepared and covalently conjugated to dendrimer scaffolds. Alternatively, the NHS-activated form of TX was covalently attached to Cy5 before linking to dendritic scaffolds (Supporting Information). After each successive addition reaction and purification, the average degree of substitution is determined using MALDI-TOF mass spectrometry (Tables S1 and S2).

Photophysical Characterization. FDN compounds were characterized using both bulk absorbance/fluorescence emission and single molecule fluorescence imaging. Absorbance spectra were obtained using a Nanodrop UV/vis spectrophotometer, and emission spectra were obtained with a Cary Eclipse Fluorescence Spectrophotometer. Single molecule imaging experiments were performed with an inverted microscope (Olympus IX-71) equipped for total internal reflection fluorescence microscopy (TIRF-M). Digital images are captured with an electron multiplying charge coupled device (EMCCD) camera (Andor). Fluorescent probes are linked to glass coverslip surfaces using specific chemical linkages via biotin−avidin affinity labeling or copper free click chemistry (Supporting Information). Glass coverslips are first functionalized with PEG/PEG−biotin followed by incubation with NeutrAvidin. FDN−biotin probes are subsequently incubated directly with PEG/PEG−biotin−NeutrAvidin surfaces, whereas FDN−DBCO probes are first conjugated with biotin-azide linkers, followed by incubation with functionalized glass surfaces. In addition to surface-based in vitro photophysical characterization, FDNs are used for immunofluorescence imaging experiments and single molecule DNA labeling and imaging (Supporting Text and Tables S3 and S4).

■ RESULTS AND DISCUSSION

FDN derivatives were synthesized using two different synthetic strategies for dye stabilization of multichromophoric systems

DOI: 10.1021/acs.analchem.5b03059
Anal. Chem. 2015, 87, 11048−11057

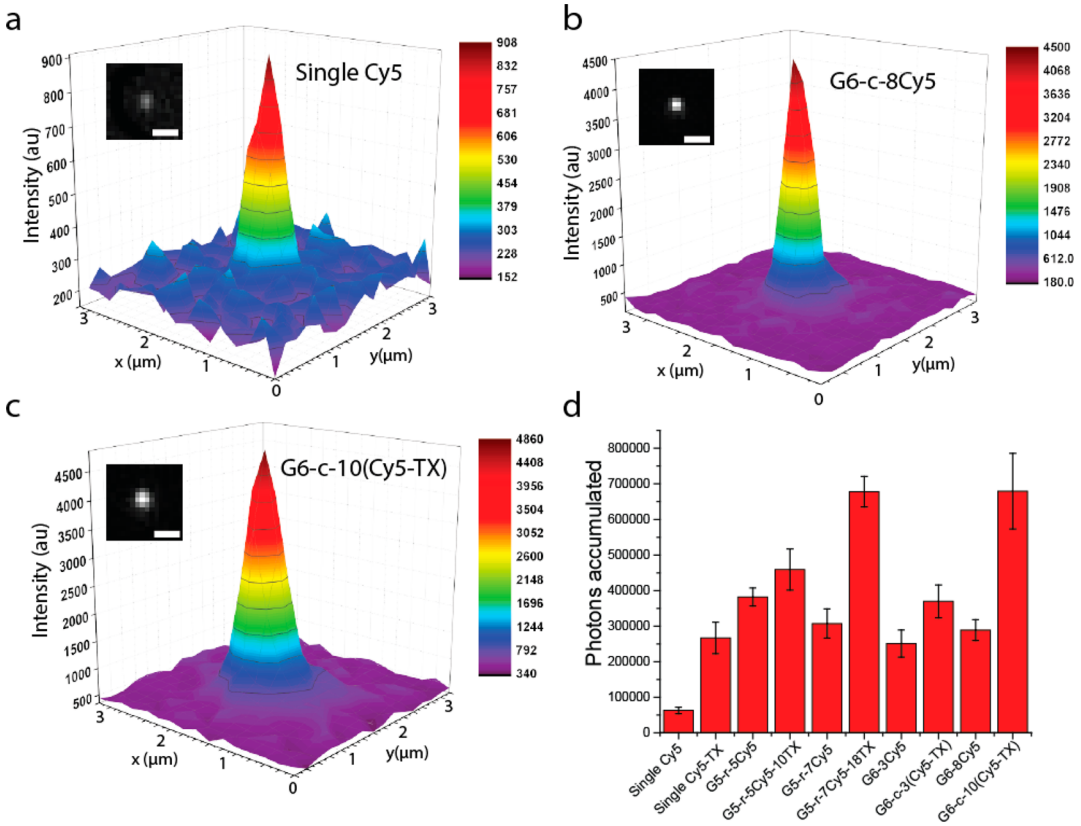

Figure 2. Single molecule characterization of fluorescent probe brightness and total accumulated photons for several different probes. (a–c) Single molecule images and fluorescence intensity plots for single Cy5, single G6–8Cy5, and G6–c-10(Cy5–TX), respectively (scale bar 1 μm). (d) Total accumulated photons for all samples in the presence of glucose oxidase/catalase and absence of reducing agents. See Tables S1 and S2 for nomenclature. For these data and unless indicated otherwise, error bars are calculated as the standard deviation of experimental data, and averages are calculated over >5 independent fields-of-view in the each sample.

(Figure 1 and Figure S1). In one class of FDN probes, multiple Cy5 dyes and multiple TX molecules are covalently conjugated onto dendrimer surfaces with control over the average stoichiometric amount of Cy5 and TX (Figure 1a). In essence, this method results in a random spatial distribution between Cy5 dyes and TX molecules on the dendrimer surface, and we refer to these probes as r-FDN–TX derivatives. For r-FDN–TX probes, we synthesized samples with a Cy5:TX dye ratio of 1:2.0 and 1:2.7 to assess the effect of increased TX loading on fluorescence emission and photostability. In a second class of FDN–TX probes, the photostabilizer TX is first conjugated to Cy5 dye, followed by direct conjugation of multiple Cy5–TX "self-healing" probes onto the dendrimer surface in variable loadings (Figure 1b). This second class of multichromophoric probes has a controlled (or local) physical spacing between Cy5 dyes and TX molecules, and we refer to these molecules as c-FDN–TX probes. In addition, biotin and/or DBCO is conjugated to dendrimer probes for surface immobilization or biomolecule labeling, and in some cases, surface charge groups are added to modulate electrostatics. In all cases, the average degree of chemical substitution can be controlled in a fairly narrow range through the reagent-to-dendrimer stoichiometry in a series of sequential chemical conjugation reactions. During synthesis, MALDI-TOF mass spectrometry analysis is used to determine the average degree of chemical substitution for each reaction step (Tables S1 and S2), and bulk photophysical properties are characterized via absorption and fluorescence emission spectra (Figure S2). Polymeric dendrimers serve as versatile molecular scaffolds for conjugation of multiple fluorescent dyes and chemical groups, thereby allowing for the tailored design and preparation of fluorescent probes with desired properties such as surface charge, dye loading, or enhanced photophysical properties via direct linkage of photostabilizers.

Using this system, we aimed to explore the role of the Cy5:TX loading ratio and physical spacing between Cy5 and the photostabilizer TX on the photophysical properties of FDN probes. It is known that the efficiency of photoinduced redox action is strongly correlated to the distance between TX and a dye molecule.[33] From this perspective, we sought to determine the role of dye-to-photostabilizer ratio on the photophysical behavior of multichromophoric systems using single molecule imaging (Figure 1c). We pursued this idea using two different approaches. For one class of molecules (r-FDN–TX), we aimed to assess the impact of increasing the loading of the photostabilizer TX on Cy5 dye emission using average stoichiometric ratios. Moreover, we also probe the role of stabilization due to putative dye–dye interactions in the absence of TX compared to photostabilization due to increasing TX loadings on a multidye dendrimer construct. In a second class of molecules (c-FDN–TX), we aimed to determine the impact of increasing the loading of Cy5–TX heterodimers on the photophysical properties of FDN derivatives, where the local physical spacing between dye and TX is fixed. Indeed, the photophysical properties of self-healing Cy5–TX molecules have been studied previously,[33,47] but it is

DOI: 10.1021/acs.analchem.5b03059
Anal. Chem. 2015, 87, 11048–11057

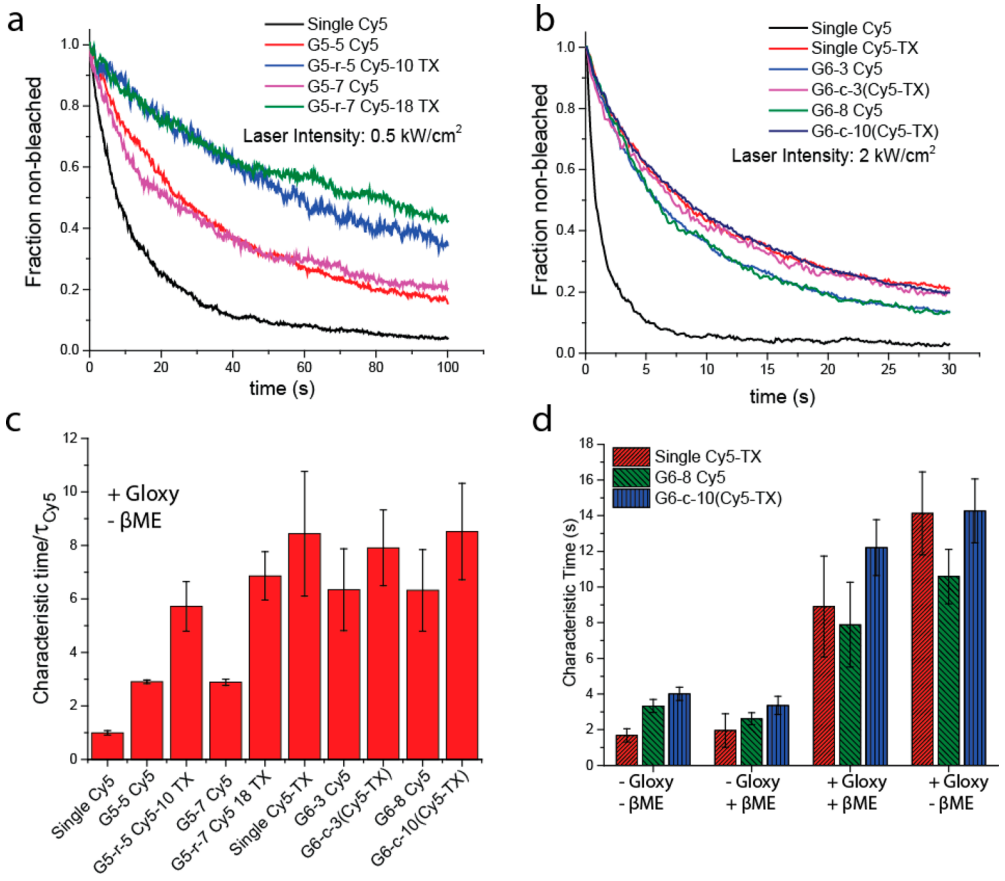

Figure 3. Single molecule characterization of probe photostability. (a) Active fraction of molecules before irreversible bleaching for single Cy5 and the random addition samples (r-FDN and r-FDN−TX) under constant laser illumination (637 nm, 0.5 kW/cm^2). (b) Active fraction of molecules before bleaching for single Cy5, single Cy5−TX, and controlled addition samples (c-FDN and c-FDN−TX) under a constant illumination (637 nm, 2 kW/cm^2). (c) Time constants obtained from a single exponential fit of fluorescent probe samples from panels a and b, normalized by the characteristic time constant for single Cy5 in +Gloxy/−BME buffer conditions. (d) Characteristic photobleaching times for selected samples under different solution conditions.

unknown how these results map onto multichromophoric systems in terms of increased brightness and enhanced photostability.

Figure 2 shows probe brightness and photon output for a wide variety of fluorescent probes. Characteristic single molecule intensity plots for a handful of selected probes are shown in Figure 2a−c, including diffraction limited images of single Cy5, G6−c-8Cy5, and G6−c-10(Cy5−TX). Here, we observe similar fluorescence intensities for G6−c-10(Cy5−TX) and G6−c-8Cy5, whereas these probes generally show a ∼4−5× increase in intensity relative to single dyes, consistent with prior data on FDNs without covalent coupling of photostabilizers.[38] The total number of accumulated photons before irreversible photobleaching is shown for all samples in Figure 2d, which reveals several interesting features for these fluorescent probes. In all cases, covalent attachment of TX leads to increases in total photon output compared to the parent "non-healed" version of the probe. Furthermore, we find a larger increase in total photon output for r-FDN−TX probes with a 1:2.7 ratio of Cy5:TX (relative to the parent r-FDN probe without TX) compared to r-FDN−TX probes with a 1:2.0 ratio Cy5:TX. These results suggest that increasing the loading of TX in r-FDN−TX probes increases total photon output for a given system, presumably by decreasing the physical spacing between dye and photostabilizer. Interestingly, we find an insignificant difference in the photon output for G6−3Cy5 compared to G6−8Cy5 probes, which suggests that dye−dye interactions and quenching likely play a major role only at very high dye loadings in this system. By creating "self-healed" versions of FDN probes such as G6−c-3(Cy5−TX) and G6−c-10(Cy5−TX), we observe a nearly ∼2× increase in the number of accumulated photons before bleaching. Importantly, these results suggest that dye−dye quenching can be suppressed in multichromophoric systems by control over the spatial arrangement of dye and photostabilizer, leading to enhanced brightness and photon output.

We next characterized the photobleaching behavior of these fluorescent probes using single molecule imaging (Figure 3). For these experiments, we immobilize the indicated molecule on a glass coverslip surface using specific chemical linkages and image the sample under continuous illumination. Next, we use image analysis software to localize and detect the number of fluorescent molecules as a function of time. In Figure 3a, we plot the "active" fraction of fluorescent probes for the random addition samples (r-FDN) as a function of time, along with single Cy5 for comparison. Similarly, Figure 3b shows transient photobleaching behavior for the controlled addition samples (c-FDN) compared to single Cy5 and single Cy5−TX. To quantify the photobleaching behavior in Figure 3a,b, transient fluorescence trajectories are fit to a single exponential decay in order to obtain a characteristic decay time. To compare the photophysical properties of probes independent of illumination

DOI: 10.1021/acs.analchem.5b03059
Anal. Chem. 2015, 87, 11048−11057

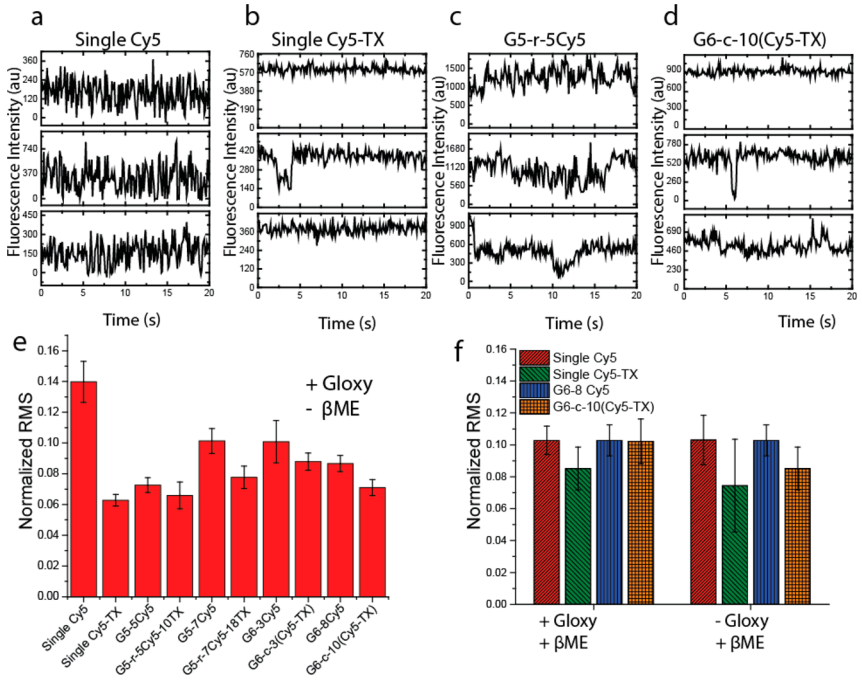

Figure 4. Single molecule characterization of transient fluorescence emission intensity. (a–d) Representative single molecule intensity trajectories for single Cy5, single Cy5–TX, G5–r-5Cy5, and G6–c-10(Cy5–TX), respectively. (e) Normalized root-mean-square intensity fluctuations for all samples in + Gloxy/-BME solution conditions. (f) Normalized root-mean-square intensity fluctuations for selected samples under two different solution conditions.

conditions, photobleaching decay times are normalized by the characteristic decay time for single Cy5 in each experiment, which effectively serves as an internal reference for these samples. Figure 3c shows normalized characteristic photobleaching times for all samples. We find that the characteristic decay times for G5–r-5Cy5–10TX and G5–r-7Cy5–18TX are much larger than their "non-healed" counterparts, with a larger increase in the 1:2.7 Cy5:TX sample compared to the 1:2.0 Cy5:TX sample, as expected. Moreover, the samples with the highest degrees of photostability are probes with "controlled" physical spacing between dye and Trolox, including single Cy5–TX, G6–c-3(Cy5–TX), and G6–c-10(Cy5–TX). Here, we observe nearly equal characteristic decay times for single Cy5–TX heterodimers or controlled structure c-FDN–TX probes. On the basis of these data, it appears that FDNs bearing multiple "self-healed" Cy5–TX probes show an increase in total photon output (or total probe brightness), albeit with a characteristic photobleaching time similar to single self-healed Cy5–TX probes.

The observation that FDNs with controlled structures bearing multiple Cy5–TX molecules exhibit similar photobleaching behavior compared to Cy5–TX heterodimers likely indicates that Trolox dominates the photophysics due to the high local concentration of TX. For this reason, FDNs with controlled structures behave similarly to Cy5–TX heterodimers in terms of time before irreversible photobleaching. Moreover, the total photon output can be increased in FDNs by conjugating multiple Cy5–TX dimers on dendrimer scaffolds, which yields an overall increased brightness per probe. In the case of c-FDN–TX probes and Cy5–TX heterodimers, the enhancements in photostability are achieved due to the photoprotective effects of the Trolox molecule. Interestingly, in the absence of photoprotectants on FDN scaffolds, there is an apparent modest increase in photostability as evidenced by an increase in time to photobleaching for FDN probes bearing multiple dyes and without Trolox. We hypothesize that dye–dye interactions could give rise to this apparent increase in photostability. In particular, it is possible that the close proximity of multiple dyes may give rise to weak coupling interactions between dyes on the underlying dendrimer scaffold, which could explain these effects.[38] Nevertheless, the increase in photostability provided by covalent addition of Trolox vastly improves photostability and the photophysical properties of dye-conjugated probes.

To characterize further the behavior of these probes, we studied the photobleaching behavior of a subset of samples under different solution conditions (Figure 3d). Unless otherwise stated, the imaging buffer consists of an enzymatic oxygen removal system (glucose oxidase/catalase, Gloxy) with no reducing agent (β-mercaptoethanol, βME) in solution. In a series of experiments, we characterized the photophysical properties of several fluorescent probes in the presence or absence of Gloxy and βME, specifically $\pm$Gloxy and $\pm\beta$ME. A particularly interesting result arises from the $-$Gloxy/$-\beta$ME condition, where we observe a nearly $\sim$2$\times$ increase in the characteristic photobleaching decay time for G6–c-10(Cy5–TX) compared to single Cy5–TX. Therefore, in the presence of oxygen, c-FDN–TX probes appear a modest increase in photostability relative to single Cy5–TX probes. The increase in photostability for c-FDN–TX probes compared to single Cy5–TX in the presence of oxygen ($-$Gloxy/$-$BME) could arise due to modest protection from the underlying dendrimer scaffold, which could aid in preventing oxygen damage in the context of dendrimer probes.

Aside from brightness and long-time photobleaching, transient fluorescence emission is a key property for single molecule imaging experiments. In particular, it is highly desirable to achieve stability in transient fluorescence emission

DOI: 10.1021/acs.analchem.5b03059
Anal. Chem. 2015, 87, 11048–11057

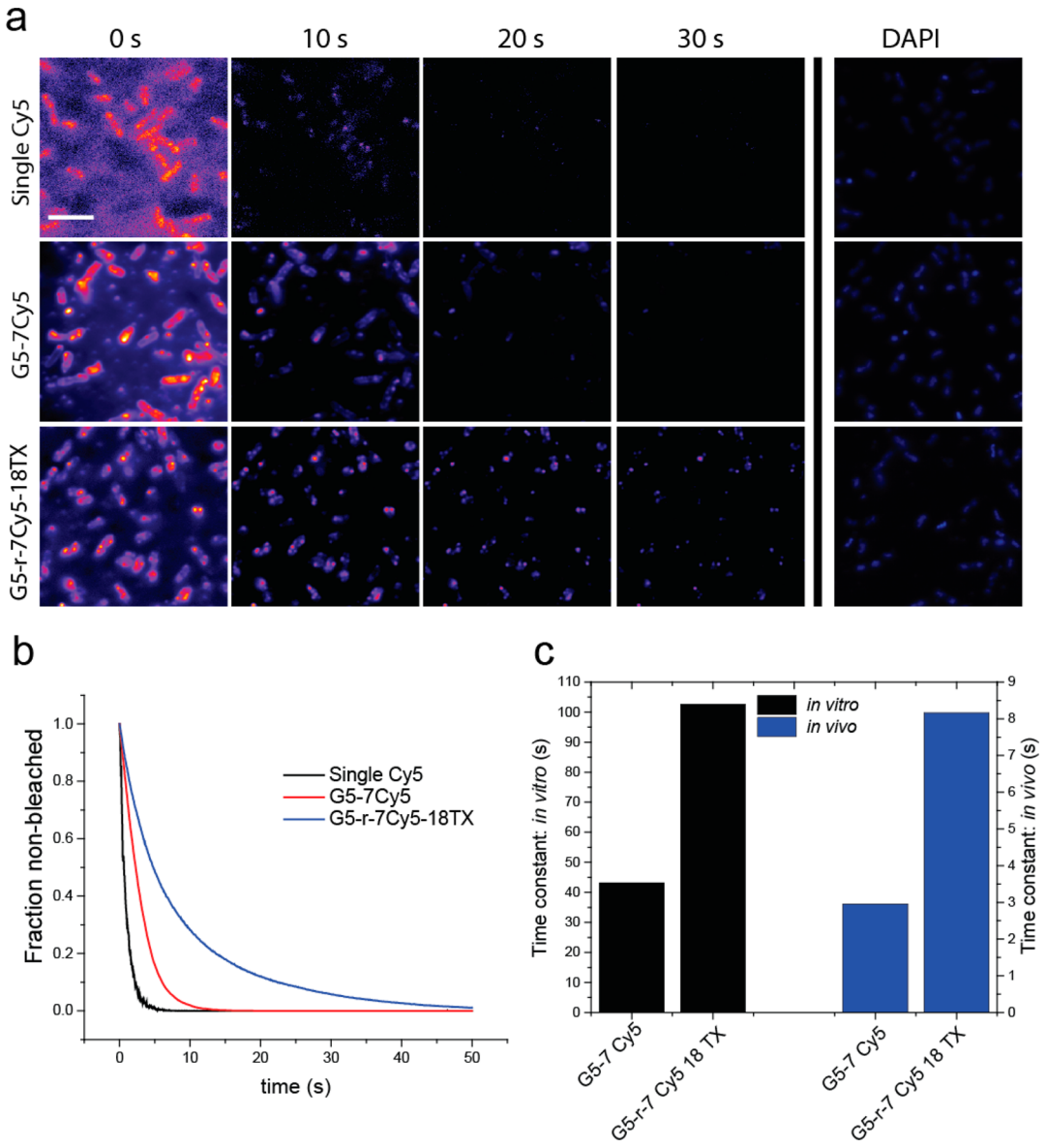

Figure 5. Bulk immunofluorescence imaging in *Escherichia coli* using FDN-labeled antibodies. (a) Immunofluorescence images of *E. coli* cells under identical illumination conditions as a function of time. For reference, a nuclear DAPI stain is shown. Scale bar: 10 μm. (b) Relative fluorescence intensity of immunolabeled cells shows transient photobleaching. (c) Photobleaching time constants from a single exponential fit for G5−7Cy5 and G5−r-7Cy5−18TX from in vivo immunofluorescence experiments and in vitro experiments shown in Figure 3a.

intensity for applications such as single molecule particle tracking, colocalization, or quantitative bioassays such as single molecule protein pull down (SiMPull).[48] In Figure 4a−d, we show representative single molecule intensity trajectories for a subset of fluorescent probes. Comparing Figure 4 panels a and b, we observe much higher stability in Cy5−TX over Cy5. In Figure 4c, we see some level of stabilization of G5−r-5Cy5 compared with Cy5, due either to dye−dye interactions or inherent stabilization due to the polymer scaffold. Finally, in Figure 4d, we see higher levels of stabilization by addition of Trolox into the structure. To quantify local transient photostability, we calculated the normalized root-mean-square deviation from the mean (RMS) of single molecule intensity until irreversible photobleaching, such that a lower value indicates a lower variation in intensity (Supporting Information). The results are shown in Figure 4e for two classes of self-healing dyes in standard buffer conditions (+Gloxy/−βME). As expected, we observe a large increase in RMS for single Cy5 compared to single Cy5−TX conjugates, which validates this approach for studying local transient photostability. For r-FDN−TX probes, we see increased levels of stabilization with higher loadings of Trolox, as expected (a difference of ∼10% for G5−5Cy5 over G5−r-5Cy5−10TX compared with ∼30% for G5−7Cy5 over G5−r-7Cy5−18TX). Moreover, the controlled structure probes G6−c-3(Cy5−TX) and G6−c-10(Cy5−TX) show only a modest stabilization in local transient fluorescence compared to the parent FDN probes without Trolox. The fairly modest enhancement in photostability for the c-FDN−TX probes can be explained in part by inherent photostabilization of dyes due to the underlying polymeric scaffold or due to dye−dye interactions, which has been observed previously.[49,50] To further explore these results, we determined the normalized RMS values for selected samples in variable solution conditions with ±Gloxy and + βME (Figure

DOI: 10.1021/acs.analchem.5b03059
Anal. Chem. 2015, 87, 11048−11057

4f). The presence of reducing agent βME in the imaging buffer is expected to provide a modest enhancement in photostability, and we indeed find that the fluctuations in fluorescence intensity are of similar magnitude for Cy5 and Cy5−TX conjugates under these conditions. Overall, these results suggest that the effect of photostabilizers is sensitive to the local environment of the dye, including the underlying dendrimer scaffold or the presence of reducing agents in solution.

In addition, we compared the photophysical performance of dendrimer probes with covalently linked Trolox to dendrimer probes without covalent TX both in the presence and absence of Trolox in solution (Figure S6). In particular, these results include characterization of the total number of accumulated photons before photobleaching, the nonbleached fraction of molecules, and the normalized RMS fluctuation value for the FDN samples with a 1:2 dye:TX labeling ratio (including the control sample with no covalent Trolox on the dendrimer). Our results show nearly identical behavior for total number of accumulated photons and time before irreversible photobleaching for dendrimer probes with covalently linked Trolox and dendrimer probes without covalent TX but with 2 mM Trolox in solution. For these samples, we generally observe a slight decrease in transient fluctuations in fluorescence upon addition of Trolox to solution. These results demonstrate that increasing the local concentration of photoprotectants via covalent conjugation greatly improves photophysical performance, which can be advantageous for experiments wherein addition of large amounts of Trolox or photoprotectant to bulk solution is not possible.

Moving beyond in vitro photophysical characterization of FDN−Trolox derivatives using SMFM, we performed several proof-of-principle imaging experiments using these probes, including bulk immunofluorescence imaging and single molecule DNA labeling experiments. In a first set of experiments, we used FDN−Trolox probes in immunofluorescence imaging of fixed bacterial cells (*Escherichia coli*). Here, we targeted glyceraldehyde phosphate dehydrogenase (GAPDH), an oxidoreductase and key enzyme in glycolysis that catalyzes the conversion of glyceraldehyde 3-phosphate (GADP) to D-1,3-bisphosphoglycerate (1,3BPG) using NAD^+ as an electron acceptor. In these experiments, we aimed to characterize the long-term photostability of FDN derivatives for bulk immunofluorescence imaging by labeling anti-GAPDH primary antibodies with single Cy5 dye, G5−7Cy5, and G5−r-7Cy5−18TX (Figure 5).

Immunofluorescence imaging results are shown in Figure 5a as a function of time, along with images of cellular DAPI stain in the same field of view, which properly overlays with the immunofluorescence images and serves as an internal reference for cells. Transient fluorescence intensities during imaging under constant illumination are shown in Figure 5b. First, these results demonstrate that FDN−TX probes can be used to label and image antibodies using a standard immunofluorescence protocol. Characteristic photobleaching trajectories show that anti-GAPDH primary antibodies labeled with FDN−Trolox derivatives generally exhibit an enhanced photostability compared to primary Abs labeled with Cy5 or FDN probes without covalent attachment of Trolox, which is consistent with the results in Figure 3. Generally speaking, this increased photostability would allow additional biological or chemical information to be extracted from immunofluorescence experiments using this set of probes. To quantify further photostability in this experiment, we determined the characteristic photobleaching decay time constants for G5−r-7Cy5−18TX and G5−7Cy5 (Figure 5c), including a comparison to the in vitro photobleaching experiments shown in Figure 3. We observe only a very small difference between the data gleaned from both experiments, which further suggests that FDN probes can be confidently used in immunofluorescence imaging experiments.

Specific labeling of target biomolecules is highly desirable for biological imaging applications. In certain cases, however, specific labeling can be challenging due to electrostatic interactions. For example, in prior work,[38] we labeled DNA oligonucleotides with FDNs containing terminal amine groups, which bear a nominal positive charge at neutral pH. In this case, specific labeling was accomplished by addition of high salt and a nonspecific blocking agent to the reaction buffer, thereby screening electrostatic interactions between the positively charged FDN probes and negatively charged DNA, which otherwise results in nonspecific binding.[38] To circumvent these requirements and to allow for facile specific labeling in a simple buffer, we synthesized FDN samples with variable surface charge to suppress electrostatic interactions between FDN probes and target DNA (Supporting Text, Tables S3 and S4, and Figure S7). In all cases, we achieve specific labeling of target DNA molecules with no evidence of aggregate formation or nonspecific interactions.

CONCLUSIONS

In this work, we expand the use of "self-healing" fluorophores from single organic dyes to multidye dendrimer nanoconjugates, which offers a new set of bright and photostable probes for single molecule fluorescence microscopy and general immunofluorescence imaging. Using two complementary synthetic strategies, we synthesized self-healing FDN probes with either average stoichiometric loading (and random spatial distribution) of Cy5 and Trolox molecules on the dendrimer surface, or with direct covalent attachment of multiple "self-healing" Cy5−Trolox conjugates. In the first strategy, we are able to modulate the average stoichiometric loading of Trolox (per dye), which leads to enhanced fluorescence stabilization upon increasing the Trolox to dye ratio. However, this strategy affords essentially no control over the spatial arrangement of dye or photostabilizer substituents, which precludes absolute control over the distance between fluorophore−protectant pairs. In addition, we only control the average stoichiometry per dendrimer using this synthetic method, which leads to distributions in the ratio of dye:TX (Figures S4 and S5).

In an alternative strategy, we synthesized multichromophoric denderimers bearing Cy5−Trolox conjugates. Interestingly, these fluorescent probes emit a large number of total photons before irreversible photobleaching, though they exhibit characteristic photobleaching times comparable to single Cy5−TX molecules, implying that a single self-healed Cy5−TX conjugate achieves a maximal amount of photostabilization, albeit only with the brightness of a single dye. In particular, G6−c-10(Cy5−TX) is an FDN probe bearing multiple Cy5−TX conjugates that shows a very large photon output, which could find applications in single molecule particle tracking experiments, allowing for precise, long-term localization for a biomolecules. However, despite the advantages of multichromophoric FDN−TX systems, it should be noted that dendrimer-based probes are larger in size (∼5 nm) compared to single organic dyes (∼1 nm).

DOI: 10.1021/acs.analchem.5b03059
Anal. Chem. 2015, 87, 11048−11057

Prior studies have examined the role of covalently linked Trolox on single fluorophores, whereas our work extends this approach to multichromophoric systems with enhanced brightness. Our results appear to be consistent with the "ping-pong" mechanism attributed to the photoprotective action of Trolox covalently localized to a single dye. Here, the triplet state of a dye is reduced by an adjacent Trolox molecule, followed by rapid reoxidation of the dye with the radical Trolox cation. This "self-healing" mechanism critically depends on the local proximity between the two molecular species. Indeed, our results show increased photoprotection upon increasing the dye:TX ratio on random addition FDN probes (r-FDN−TX probes). However, it is possible that a combination of photostabilization dye to TX and dye−dye interactions results in increased photoprotection in the 1:2.7 dye:TX sample. On the other hand, the controlled addition samples (c-FDN−TX) allow for independently changing dye loading while maintaining a constant TX:dye ratio and a constant (local) physical spacing between dye and Trolox. For these samples, we generally observe an increase in the total number of accumulated photons due to an increased dye loading, despite minor differences between the photostability for G6−c-3(Cy5−TX) and G6−c-10(Cy5−TX) samples.

In conclusion, we synthesized and characterized two distinct classes of "self-healing" multichromophoric dendrimers. By linking Trolox directly to an organic dye before covalent attachment to a dendrimer, we avoid distributions in the ratio of TX:dye with control over the average stoichiometric loading of Cy5−TX heterodimers on dendritic scaffolds. This synthesis scheme inherently leads to variations in photophysical properties within a batch of fluorescent probes, which precludes use in applications such as single molecule Forster resonance energy transfer (smFRET) requiring quantitative knowledge of dye number and spatial distribution. In future work, these issues can be overcome by designing a structurally defined multidye probe system allowing for precise control over dye attachment in the absence of the underlying dendritic scaffold.

■ ASSOCIATED CONTENT

Supporting Information

The Supporting Information is available free of charge on the ACS Publications website at DOI: 10.1021/acs.analchem.5b03059.

Text describing synthesis and chemical characterization of dendrimer probes, including mass spectrometry and ^{1}H NMR data, and methods for single molecule fluorescence microscopy. Supplementary tables (Tables S1−S4) providing chemical characterization data for dendrimers and PCR reaction conditions. Supplementary Figures (S1−S7) providing additional control experiments for single molecule characterization of FDN probes (PDF).

■ AUTHOR INFORMATION

Corresponding Author

*Charles M. Schroeder. Address: Department of Chemical and Biomolecular Engineering University of Illinois at Urbana−Champaign 109 Roger Adams Laboratory 600 South Mathews Avenue, Urbana, IL 61801. Email: cms@illinois.edu. Phone: (217) 333-3906.

Notes

The authors declare no competing financial interest.

■ ACKNOWLEDGMENTS

This work was supported by a Packard Fellowship from the David and Lucile Packard Foundation for CMS and an NIH Molecular Biophysics Training Grant (5T32GM008276-25) for DTR. We thank Utsav Agrawal, Danielle J. Mai, Luke Cuculis, and Eric M. Johnson-Chavarria for useful discussions and for assistance with immunofluorescence and imaging experiments.

■ REFERENCES

(1) Selvin, P. R.; Ha, T. *Single-Molecule Techniques: A Laboratory Manual*; Cold Spring Harbor Laboratory Press: New York, 2008.
(2) Xie, X. S.; Choi, P. J.; Li, G.-W.; Lee, N. K.; Lia, G. *Annu. Rev. Biophys.* **2008**, *37* (1), 417−444.
(3) Huang, B.; Babcock, H.; Zhuang, X. *Cell* **2010**, *143* (7), 1047−1058.
(4) Agrawal, U.; Reilly, D. T.; Schroeder, C. M. *Curr. Opin. Biotechnol.* **2013**, *24* (4), 646−653.
(5) Levitus, M.; Ranjit, S. *Q. Rev. Biophys.* **2011**, *44* (01), 123−151.
(6) Ha, T.; Tinnefeld, P. *Annu. Rev. Phys. Chem.* **2012**, *63* (1), 595−617.
(7) Basche, T.; Kummer, S.; Brauchle, C. *Nature* **1995**, *373*, 132.
(8) Blanchard, S. C.; Kim, H. D.; Gonzalez, R. L.; Puglisi, J. D.; Chu, S. *Proc. Natl. Acad. Sci. U. S. A.* **2004**, *101* (35), 12893−12898.
(9) Stennett, E. M. S.; Ciuba, M. A.; Levitus, M. *Chem. Soc. Rev.* **2014**, *43* (4), 1057.
(10) Rentsch, S. K.; Danielius, R. V.; Gadonas, R. A. *Chem. Phys. Lett.* **1981**, *84* (3), 450−453.
(11) Yip, W.-T.; Hu, D.; Yu, J.; Vanden Bout, D. A.; Barbara, P. F. *J. Phys. Chem. A* **1998**, *102* (39), 7564−7575.
(12) Ha, T.; Enderle, T.; Chemla, D. S.; Selvin, P. R.; Weiss, S. *Chem. Phys. Lett.* **1997**, *271*, 1−5.
(13) Zondervan, R.; Kulzer, F.; Orlinskii, S. B.; Orrit, M. *J. Phys. Chem. A* **2003**, *107* (35), 6770−6776.
(14) Dempsey, G. T.; Bates, M.; Kowtoniuk, W. E.; Liu, D. R.; Tsien, R. Y.; Zhuang, X. *J. Am. Chem. Soc.* **2009**, *131* (51), 18192−18193.
(15) Rust, M. J.; Bates, M.; Zhuang, X. *Nat. Methods* **2006**, *3* (10), 793−796.
(16) Heilemann, M.; van de Linde, S.; Schüttpelz, M.; Kasper, R.; Seefeldt, B.; Mukherjee, A.; Tinnefeld, P.; Sauer, M. *Angew. Chem., Int. Ed.* **2008**, *47* (33), 6172−6176.
(17) Vaughan, J. C.; Dempsey, G. T.; Sun, E.; Zhuang, X. *J. Am. Chem. Soc.* **2013**, *135* (4), 1197−1200.
(18) Zheng, Q.; Juette, M. F.; Jockusch, S.; Wasserman, M. R.; Zhou, Z.; Altman, R. B.; Blanchard, S. C. *Chem. Soc. Rev.* **2014**, *43*, 1044−1056.
(19) Harada, Y.; Sakurada, K.; Aoki, T.; Thomas, D. D.; Yanagida, T. *J. Mol. Biol.* **1990**, *216*, 49−68.
(20) Aitken, C. E.; Marshall, R. A.; Puglisi, J. D. *Biophys. J.* **2008**, *94* (5), 1826−1835.
(21) Hübner, C. G.; Renn, A.; Renge, I.; Wild, U. P. *J. Chem. Phys.* **2001**, *115* (21), 9619.
(22) Weston, K. D.; Carson, P. J.; DeAro, J. A.; Buratto, S. K. *Chem. Phys. Lett.* **1999**, *308* (1), 58−64.
(23) Yanagida, T.; Nakase, M.; Nishiyama, K.; Oosawa, F. *Nature* **1984**, *307*, 58−60.
(24) Blanchard, S. C.; Gonzalez, R. L.; Kim, H. D.; Chu, S.; Puglisi, J. D. *Nat. Struct. Mol. Biol.* **2004**, *11* (10), 1008−1014.
(25) Grunwell, J. R.; Glass, J. L.; Lacoste, T. D.; Deniz, A. A.; Chemla, D. S.; Schultz, P. G. *J. Am. Chem. Soc.* **2001**, *123* (18), 4295−4303.
(26) Widengren, J.; Chmyrov, A.; Eggeling, C.; Löfdahl, P.-Å.; Seidel, C. A. M. *J. Phys. Chem. A* **2007**, *111* (3), 429−440.
(27) Rasnik, I.; McKinney, S. A.; Ha, T. *Nat. Methods* **2006**, *3* (11), 891−893.
(28) Vogelsang, J.; Kasper, R.; Steinhauer, C.; Person, B.; Heilemann, M.; Sauer, M.; Tinnefeld, P. *Angew. Chem., Int. Ed.* **2008**, *47* (29), 5465−5469.

DOI: 10.1021/acs.analchem.5b03059
Anal. Chem. 2015, 87, 11048−11057

(29) Dave, R.; Terry, D. S.; Munro, J. B.; Blanchard, S. C. *Biophys. J.* **2009**, *96* (6), 2371−2381.
(30) Cordes, T.; Maiser, A.; Steinhauer, C.; Schermelleh, L.; Tinnefeld, P. *Phys. Chem. Chem. Phys.* **2011**, *13* (14), 6699.
(31) Campos, L. A.; Liu, J.; Wang, X.; Ramanathan, R.; English, D. S.; Muñoz, V. *Nat. Methods* **2011**, *8* (2), 143−146.
(32) Alejo, J. L.; Blanchard, S. C.; Andersen, O. S. *Biophys. J.* **2013**, *104* (11), 2410−2418.
(33) Altman, R. B.; Terry, D. S.; Zhou, Z.; Zheng, Q.; Geggier, P.; Kolster, R. A.; Zhao, Y.; Javitch, J. A.; Warren, J. D.; Blanchard, S. C. *Nat. Methods* **2011**, *9* (1), 68−71.
(34) Tinnefeld, P.; Cordes, T. *Nat. Methods* **2012**, *9* (5), 426−427.
(35) Zheng, Q.; Jockusch, S.; Zhou, Z.; Altman, R. B.; Warren, J. D.; Turro, N. J.; Blanchard, S. C. *J. Phys. Chem. Lett.* **2012**, *3* (16), 2200−2203.
(36) van der Velde, J. H. M.; Ploetz, E.; Hiermaier, M.; Oelerich, J.; de Vries, J. W.; Roelfes, G.; Cordes, T. *ChemPhysChem* **2013**, *14* (18), 4084−4093.
(37) Altman, R. B.; Zheng, Q.; Zhou, Z.; Terry, D. S.; Warren, J. D.; Blanchard, S. C. *Nat. Methods* **2012**, *9* (5), 428−429.
(38) Kim, Y.; Kim, S. H.; Tanyeri, M.; Katzenellenbogen, J. A.; Schroeder, C. M. *Biophys. J.* **2013**, *104* (7), 1566−1575.
(39) Caminade, A.-M.; Hameau, A.; Majoral, J.-P. *Chem. - Eur. J.* **2009**, *15* (37), 9270−9285.
(40) Swallen, S. F.; Kopelman, R.; Moore, J. S.; Devadoss, C. *J. Mol. Struct.* **1999**, *485*, 585−597.
(41) Hernando, J.; van der Schaaf, M.; van Dijk, E. M. H. P.; Sauer, M.; García-Parajó, M. F.; van Hulst, N. F. *J. Phys. Chem. A* **2003**, *107* (1), 43−52.
(42) Hofkens, J.; Maus, M.; Gensch, T.; Vosch, T.; Cotlet, M.; Köhn, F.; Herrmann, A.; Müllen, K.; De Schryver, F. *J. Am. Chem. Soc.* **2000**, *122* (38), 9278−9288.
(43) Vosch, T.; Hofkens, J.; Cotlet, M.; Köhn, F.; Fujiwara, H.; Gronheid, R.; Van Der Biest, K.; Weil, T.; Herrmann, A.; Müllen, K.; et al. *Angew. Chem.* **2001**, *113* (24), 4779−4784.
(44) Mujumdar, R. B.; Ernst, L. A.; Mujumdar, S. R.; Lewis, C. J.; Waggoner, A. S. *Bioconjugate Chem.* **1993**, *4* (2), 105−111.
(45) Agard, N. J.; Prescher, J. A.; Bertozzi, C. R. *J. Am. Chem. Soc.* **2004**, *126* (46), 15046−15047.
(46) Baskin, J. M.; Prescher, J. A.; Laughlin, S. T.; Agard, N. J.; Chang, P. V.; Miller, I. A.; Lo, A.; Codelli, J. A.; Bertozzi, C. R. *Proc. Natl. Acad. Sci. U. S. A.* **2007**, *104* (43), 16793−16797.
(47) van der Velde, J. H. M.; Oelerich, J.; Huang, J.; Smit, J. H.; Hiermaier, M.; Ploetz, E.; Herrmann, A.; Roelfes, G.; Cordes, T. *J. Phys. Chem. Lett.* **2014**, *5*, 3792−3798.
(48) Jain, A.; Liu, R.; Ramani, B.; Arauz, E.; Ishitsuka, Y.; Ragunathan, K.; Park, J.; Chen, J.; Xiang, Y. K.; Ha, T. *Nature* **2011**, *473* (7348), 484−488.
(49) Bai, Y.; Xing, H.; Vincil, G. A.; Lee, J.; Henderson, E. J.; Lu, Y.; Lemcoff, N. G.; Zimmerman, S. C. *Chem. Sci.* **2014**, *5* (7), 2862.
(50) Yang, S. K.; Shi, X.; Park, S.; Ha, T.; Zimmerman, S. C. *Nat. Chem.* **2013**, *5* (8), 692−697.

DOI: 10.1021/acs.analchem.5b03059
Anal. Chem. 2015, 87, 11048−11057